Interaction of an aluminum atom with a closed subshell metal atom: Spectroscopic analysis of AlZn

Jane M. Behm, Thorsten Blume, and Michael D. Morse

Citation: J. Chem. Phys. **101**, 5454 (1994); doi: 10.1063/1.467334
View online: http://dx.doi.org/10.1063/1.467334
View Table of Contents: http://jcp.aip.org/resource/1/JCPSA6/v101/i7
Published by the American Institute of Physics.

Interaction of an aluminum atom with a closed subshell metal atom: Spectroscopic analysis of AlZn

Jane M. Behm,[a] Thorsten Blume,[b] and Michael D. Morse
Department of Chemistry, University of Utah, Salt Lake City, Utah 84112

(Received 25 March 1994; accepted 24 June 1994)

Resonant two-photon ionization spectroscopy has been employed to investigate diatomic AlZn produced by laser vaporization of a 1:2 Al:Zn alloy target disk in a supersonic expansion of helium. Several discrete transitions are reported in the energy range from 18 400 to 19 100 cm^{-1}. Most of these are assigned as members of the $B\ ^2\Pi \leftarrow X\ ^2\Pi$ system, although an isolated band has been observed and assigned as the 2-0 band of the $A\ \Omega'=0.5 \leftarrow X\ ^2\Pi_{1/2}$ system. A pair of strongly mixed levels are identified as resulting from a homogeneous spin–orbit perturbation between the $A\ \Omega=0.5$, $v'=3$ and the $B\ ^2\Pi_{1/2}$, $v'=1$ levels, and the perturbation matrix element has been deduced to be 8.11 cm^{-1} for $^{27}Al^{64}Zn$, 8.23 cm^{-1} for $^{27}Al^{66}Zn$. The ground state has been unambiguously identified as a $^2\Pi_r$ state with a bond length of 2.6957±0.0004 Å. Comparisons to the results of the preceding article on the spectroscopy of AlCa are also provided, along with a discussion of the chemical bonding in AlZn in relation to AlCa, AlAr, and AlKr.

I. INTRODUCTION

The spectroscopic analysis of AlZn presented in this paper provides another link in the spectroscopic investigation of the transition metal aluminides, which we began with studies of AlCu (Ref. 1) and AlNi,[2] and have now continued with studies of AlCa (Ref. 3) and AlZn. As stated more explicitly in the preceding paper on the spectroscopy of AlCa,[3] the purpose of this series of studies is to investigate the chemical bonding which results between a simple p-block main group element, aluminum, and the $3d$ series of transition metal atoms. Although the bonding in AlZn and AlCa is expected to arise from the same basic type of interaction (a $4s^2_{Ca,Zn}$ atom interacting with a $3p^1_{Al}$ atom), the spectra recorded for the two diatomic molecules are quite different in their details.

As will be shown, the ground state bonding in the two diatomic molecules is indeed similar, with the favorable $p\pi$ orientation of the Al atom resulting in $^2\Pi_r$ ground states for both molecules. The differences between the spectra recorded for the two molecules therefore reflect differences in the accessible excited electronic states. A glance at the excited states of atomic calcium shows that the $4s^13d^1$, $^{1,3}D$ and $4s^14p^1$, $^{1,3}P^0$ states all lie in the range of 15 000–24 000 cm^{-1} above the $4s^2$, ^1S ground state, while in zinc the first excited state is $3d^{10}4s^14p^1$, $^3P^0$, lying approximately 32 500 cm^{-1} above ground state atoms (the isoconfigurational $3d^{10}4s^14p^1$, $^1P^0$ state lies even higher in energy, at 46 745 cm^{-1}).[4] Thus it may be expected that the spectrum of AlCa will display a greater number of band systems extending further to the red than does the spectrum of AlZn. This is precisely what is found in the present study; only two distinct excited states of AlZn have been identified, and spectra have only been found in the limited region from 18 400 to 19 100 cm^{-1}, although the regions from 17 500 cm^{-1} to nearly 24 000 cm^{-1} and from 26 000 to 29 800 cm^{-1} were carefully searched.

From the spectroscopic analysis of AlZn we hope to obtain as much information as possible, despite the absence of any prior experimental or theoretical studies on this molecule. Apart from discovering any periodic trends which may exist, the study of the transition metal aluminides is aimed at affording insights into the forces which exist between atoms of these elements, which may in turn prove beneficial in understanding the properties of the bulk alloys.

Section II presents a description of the experimental methods employed in this study while Sec. III presents the results obtained for AlZn. In Sec. IV these are interpreted and discussed in relation to the preceding results on AlCa. Section V then concludes the article with a summary of our most important findings.

II. EXPERIMENT

Diatomic AlZn was spectroscopically investigated in a resonant two-photon ionization apparatus that is described in detail in the preceding paper.[3] For brevity's sake, only the experimental aspects unique to AlZn will be described here. The 1:2 molar ratio Al:Zn alloy was prepared by heating a mixture of the pure elements in an evacuated quartz tube using a natural gas flame. The metals melted at approximately 600 °C, creating a homogeneous metal alloy which was subsequently turned on a lathe to produce a flat surface. Although this sample disk was more homogeneous than the AlCa metal target disk employed in the previous study,[3] it was also somewhat harder, and the AlZn molecular beam was more difficult to produce. A sufficient number of AlZn molecules was generated by using a higher vaporization laser fluence and, more importantly, higher backing pressures of helium (180 psi vs 80 psi). The excitation photon in the two-photon process was supplied by either frequency doubling (as described in the preceding paper)[3] the fundamental light produced by a dye laser pumped by the second harmonic radiation (532 nm) of a Nd:YAG laser, or by using the

[a]Kodak Fellow.
[b]Present address: Braunschweig Universität, Germany.

 0021-9606/94/101(7)/5454/10/$6.00

fundamental radiation produced by the dye laser pumped by the third harmonic of the Nd:YAG laser (355 nm). The second, ionizing photon was supplied in all scans by a fixed frequency excimer laser operating on KrF (248 nm, 5.0 eV).

High resolution analyses and excited state lifetimes were obtained as described for AlCa.[3] Since all of the transitions observed in AlZn fell within the limits of the I_2 atlas,[5] Raman shifting in H_2 was not necessary for calibration. The optical spectra of $^{27}Al^{64}Zn$ (48.89% natural abundance), $^{27}Al^{66}Zn$ (27.81%), $^{27}Al^{67}Zn$ (4.11%), and $^{27}Al^{68}Zn$ (18.56%) were recorded by specifically monitoring the ion signal at masses 91, 93, 94, and 95 as a function of dye laser frequency.

III. RESULTS

A. Low resolution spectrum

Diatomic AlZn was investigated in two energy regions using low resolution ($\approx$0.8 cm^{-1}) resonant two-photon ionization (R2PI) spectroscopy. The ultraviolet energy regime was initially chosen for investigation because the first excited separated atom limit $[Al(3s^24s^1,{}^2S_{1/2})+Zn(3d^{10}4s^2,{}^1S_0)]$ lies more than 25 000 cm^{-1} above the ground state separated atom limit.[4] To investigate this region, the LDS dyes were scanned from 13 000 cm^{-1} to nearly 14 900 cm^{-1}, and were frequency-doubled using an angle-tuned, servo-tracked KD*P doubling crystal to create ultraviolet light in the 26 000–29 800 cm^{-1} range. The AlZn molecules were subjected to both the fundamental and the ultraviolet radiation, but no electronic transitions were observed.

The energy region from 17 500 to nearly 24 000 cm^{-1} was also scanned, using the fundamental radiation from coumarin 540A, 500, 480, 460, 440, and stilbene 420 laser dyes for excitation. Several vibronic bands were located in the range from 18 400 to 19 100 cm^{-1}, while base line prevailed elsewhere. Using a rather low vaporization laser fluence a cold spectrum is obtained, as depicted in the lower portion of Fig. 1 for the predominant isotopic species, $^{27}Al^{64}Zn$. Although vibrational progressions are not immediately obvious in this spectrum, the measurement of excited state lifetimes and the rotational analyses of the individual bands demonstrates that the red-shaded bands at 18 506, 18 891, and 19 083 cm^{-1} correspond to the 0-0, 2-0, and 3-0 bands of a $^2\Pi_{1/2}\leftarrow{}^2\Pi_{1/2}$ system, which we designate as the $B\leftarrow X$ system. Measured upper state lifetimes of these bands are 197±5 ns ($v'=0$) and 165±44 ns ($v'=2$). Assuming that the decay is governed by fluorescence back to the ground state, this corresponds to a fairly large absorption oscillator strength of $f\approx0.02$, indicative of a spin-allowed transition. The $v'=1$ level of the $B\ ^2\Pi_{1/2}$ state appears to be strongly perturbed by another state, which gains intensity through this interaction, resulting in two strong bands originating from the $v''=0$ level of the $X\ ^2\Pi_{1/2}$ state observed at 18 690 and 18 707 cm^{-1}. Excluding the 1-0 band from a vibronic fit and including only the 0-0, 2-0, and 3-0 bands which were measured in high resolution, values of $\omega_e' = 193.54$ cm^{-1} and $\omega_e'x_e' = 0.28$ cm^{-1} are obtained for the $B\ ^2\Pi_{1/2}$ state of $^{27}Al^{64}Zn$.

In addition to these bands originating from the $X\ ^2\Pi_{1/2}$ state, an additional set of weaker features appear at 18 606, 18 802, and 18 993 cm^{-1}. These are considerably enhanced in the upper panel of Fig. 1, which displays the low-resolution spectrum collected under conditions employing a higher vaporization laser fluence, resulting in a warmer spectrum. On the basis of rotationally resolved work reported below, these red-shaded bands are assigned as the 0-0, 1-0, and 2-0 bands of the analogous $B\ ^2\Pi_{3/2}\leftarrow X\ ^2\Pi_{3/2}$ subsystem. Finally, a strongly blue-shaded feature at 18 424 cm^{-1} in the cold spectrum is assigned as accessing an entirely different $\Omega'=0.5$ excited state located at lower energies, termed the $A\ \Omega=0.5$ state.

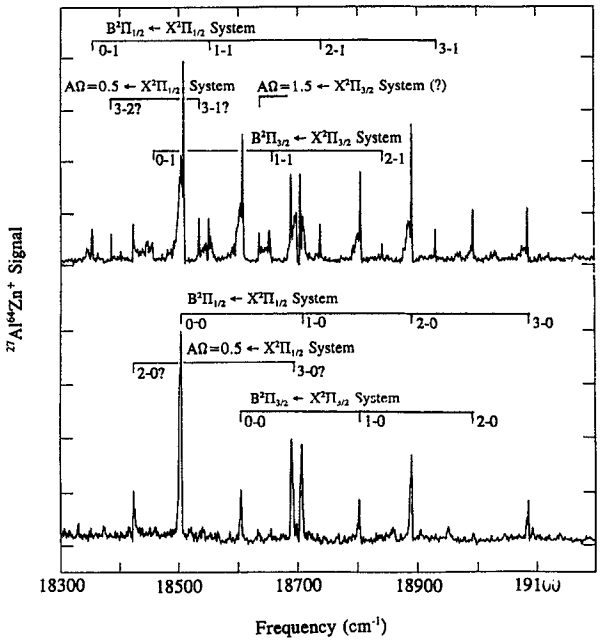

FIG. 1. Low resolution resonant two-photon ionization spectra of the $A\ \Omega=0.5\leftarrow X\ ^2\Pi_{1/2}$, $B\ ^2\Pi_{1/2}\leftarrow X\ ^2\Pi_{1/2}$, and $B\ ^2\Pi_{3/2}\leftarrow X\ ^2\Pi_{3/2}$ band systems of jet-cooled $^{27}Al^{64}Zn$, recorded using Coumarin 500 and 540A laser dyes for excitation in conjunction with KrF excimer radiation for photoionization. The upper portion of the figure was collected at higher vaporization powers than the lower portion resulting in a hotter, more congested spectrum.

The enhancement of the $B\ ^2\Pi_{3/2}\leftarrow X\ ^2\Pi_{3/2}$ bands in the warmer spectrum displayed in the upper portion of Fig. 1 allowed the 0-0, 1-0, and 2-0 bands to be rotationally resolved, allowing fitted values of $\omega_e' = 201.96$ cm^{-1} and $\omega_e'x_e' = 2.84$ cm^{-1} for the $B\ ^2\Pi_{3/2}$ state to be determined. The warmer spectrum also allows hot bands ($v''=1$) associated with the $B\ ^2\Pi_{1/2,3/2}\leftarrow X\ ^2\Pi_{1/2,3/2}$ system to be observed, permitting $\Delta G''_{1/2}$ to be fairly well estimated as 153.4 ±0.7 cm^{-1} and 154.5±2.3 cm^{-1} for the $X\ ^2\Pi_{1/2}$ and $X\ ^2\Pi_{3/2}$ states, respectively. In addition, this study finds the v'-0 bands of the $B\ ^2\Pi_{3/2}\leftarrow X\ ^2\Pi_{3/2}$ system to lie on average 101 cm^{-1} higher in frequency than the corresponding bands of the $B\ ^2\Pi_{1/2}\leftarrow X\ ^2\Pi_{1/2}$ system, implying an increase in the spin–orbit constant, A, by 101 cm^{-1} upon electronic excitation. Assuming that the ground state spin–orbit constant is similar to that of AlCa (65.2 cm^{-1}),[3] the excited state spin–orbit constant is approximately 166 cm^{-1}. This large increase in the spin–orbit constant is evidence for a *significant con-*

TABLE I. Vibronic bands of $^{27}Al^{64}Zn$.[a]

System	Band	Observed frequency (cm^{-1})	Isotope shift (cm^{-1})[b]	Lifetime (ns)
$A\ \Omega=0.5 \leftarrow X\ ^2\Pi_{1/2}$	2-0	18 424.294 5[b]	−2.853 5(38)[c,d]	977(244)[d]
$A\ \Omega=1.5 \leftarrow X\ ^2\Pi_{3/2}$(?)	2-0(?)	18 634.37	−3.92	
$B\ ^2\Pi_{1/2} \leftarrow X\ ^2\Pi_{1/2}$	0-0	18 506.035 0[b]	−0.265 0(40)[c,d]	197(5)[d]
	2-0	18 891.403 9[b]	−1.803 7(50)[c,d]	165(44)[d]
	3-0	19 083.237 1[b]	−2.703 4 (40)[c]	
	0-1	18 352.66	0.31	
	2-1	18 739.23	−1.19	
	3-1	18 928.53	−2.16	
$B\ ^2\Pi_{3/2} \leftarrow X\ ^2\Pi_{3/2}$	0-0	18 605.892 6[b]	−0.506 8(46)[c,d]	247(17)[d]
	1-0	18 802.174 1[b]	−0.997 9(19)[c,d]	
	2-0	18 992.773 4[b]	−1.85	
	0-1	18 446.88	0.00	
	1-1	18 650.81	−0.13	
	2-1	18 839.78	−1.66	
Perturbed $C \leftarrow X\ ^2\Pi_{1/2}$	C-0	18 690.271 0[b]	−2.937 9(37)[c,d]	301(32)[d]
	C-1	18 532.30	−1.60	
	C-2	18 383.34	−1.07	
Perturbed $D \leftarrow X\ ^2\Pi_{1/2}$	D-0	18 706.533 5[b]	−2.185 4(40)[c,d]	259(23)[d]
	D-1	18 549.09	−1.60	

[a]Vibronic bands were fitted to the formula $\nu = \nu_{oo} + \omega'_e v' - \omega'_e x'_e (v'^2 + v') - v''\Delta G''_{1/2}$ for $v''=0,1$. For the $B \leftarrow X$ systems the three bands measured in high resolution were fitted to extract ω'_e and $\omega'_e x'_e$, giving the values provided in Table III, while all six bands were fitted to extract $\Delta G''_{1/2}$.
[b]Isotope shifts are defined as $\nu(^{27}Al^{66}Zn) - \nu(^{27}Al^{64}Zn)$.
[c]Measured in high resolution as a band origin, with absolute calibration based on the I_2 atlas.
[d]Quantities in parentheses represent 1σ error limits, and correspond to the last digit(s) in the reported values.

tribution in the $B\ ^2\Pi$ state from the $4s^1 4p^1$ configuration of Zn (which has an atomic spin–orbit parameter, ζ_{4p}, of 386 cm^{-1}).[4,6]

Finally, it is believed that these conditions have allowed a band of the $A\ \Omega'=1.5 \leftarrow X\ ^2\Pi_{3/2}$ system to be observed at 18 634 cm^{-1}. Although this has not been confirmed through rotational analysis because of the weak intensity of the feature, no other reasonable assignment of this undoubtedly blue-shaded feature is apparent. A listing of all observed vibronic bands is provided in Table I along with their respective isotope shifts and measured excited state lifetimes.

The rotational analysis of six bands involving the $v''=0$ level of the $X\ ^2\Pi_{1/2}$ state and three bands involving the $v''=0$ level of the $X\ ^2\Pi_{3/2}$ state has allowed precise values of $B''_0 = 0.122\ 47 \pm 0.000\ 06$ and $0.122\ 06 \pm 0.000\ 04$ to be determined for the $X\ ^2\Pi_{1/2}$ and $X\ ^2\Pi_{3/2}$ components, respectively, for the predominant isotopic modification, $^{27}Al^{64}Zn$. Averaging and inverting these values then results in a ground state bond length of $^{27}Al^{64}Zn$ of $r''_0(X\ ^2\Pi) = 2.6957 \pm 0.0004$ Å.

B. Rotationally resolved spectra of the $B\ ^2\Pi_{1/2} \leftarrow X\ ^2\Pi_{1/2}$ band system

The unperturbed 0-0, 2-0, and 3-0 bands of the $B\ ^2\Pi_{1/2} \leftarrow X\ ^2\Pi_{1/2}$ band system had sufficient intensity to allow rotationally resolved spectra to be collected and analyzed. Figure 2 displays a high resolution (0.04 cm^{-1}) scan over the 0-0 band of the $B\ ^2\Pi_{1/2} \leftarrow X\ ^2\Pi_{1/2}$ system, which is similar in structure to the 2-0 and 3-0 bands. The vibrational assignment of the band is confirmed by the small isotope shift $[\nu(^{27}Al^{66}Zn) - \nu(^{27}Al^{64}Zn) = -0.265\ cm^{-1}]$ which is characteristic of origin bands. As was expected from the red-shading of this feature in the low resolution spectrum (see the upper panel of Fig. 1), the band exhibits a band head in the R branch. In addition, a weak Q branch is present along with an extended series of P lines. Splitting of the higher P lines is evident in the spectrum, and close inspection reveals that the higher R lines are split as well. This is due to Λ-doubling, which in principle can exist in both the upper and lower states.

Given that the only reasonable alternatives for the

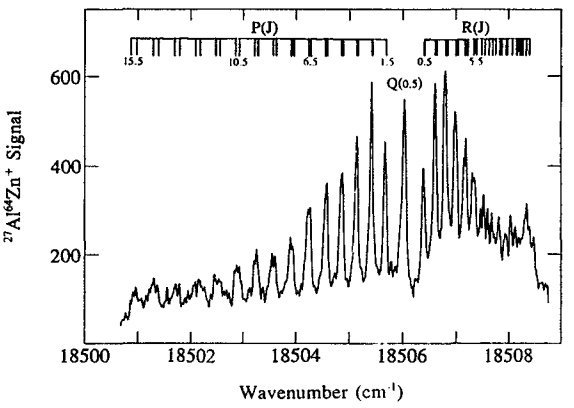

FIG. 2. Rotationally resolved scan over the *0-0 band of the* $B\ ^2\Pi_{1/2} \leftarrow X\ ^2\Pi_{1/2}$ system. The slight bandhead in the R branch indicates that the bond lengthens upon electronic excitation.

ground state are the $^2\Sigma^+$, $^2\Pi_{1/2}$, and $^2\Pi_{3/2}$ states that derive from the ground states of the atoms, the assignment of the system as a $^2\Pi_{1/2}\leftarrow X\ ^2\Pi_{1/2}$ transition follows without question. Assuming that the spin–rotation constants, γ, of the upper and lower $^2\Sigma^+$ states are small, a $^2\Sigma^+(b)\leftarrow{}^2\Sigma^+(b)$ assignment may be ruled out by the presence of a Q branch and the requirement of half-integer rotational quantum numbers in fitting the P, Q, and R structure of the band. Likewise, the observation of only three main branches instead of the four main branches expected for a $^2\Pi(a)\leftarrow{}^2\Sigma^+(b)$ or a $^2\Sigma(b)\leftarrow{}^2\Pi(a)$ system rules out the possibility of a transition between $^2\Pi(a)$ and $^2\Sigma(b)$ states. At low rotational levels the possibility of a $^2\Pi(b)$ state in a heavy molecule such as AlZn may be dismissed because the expected spin–orbit splitting, A, is much larger than the expected rotational constant, B, so the only remaining possible assignments for the transition are $^2\Pi_{1/2}\leftarrow X\ ^2\Pi_{1/2}$, $^2\Pi_{3/2}\leftarrow X\ ^2\Pi_{3/2}$, $^2\Delta_{3/2}\leftarrow X\ ^2\Pi_{1/2}$, and $^2\Delta_{5/2}\leftarrow X\ ^2\Pi_{3/2}$. All of these are expected to have P, Q, and R branches, but the observation of $R(0.5)$ and $P(1.5)$ in the spectrum implies $\Omega'=\Omega''=0.5$, providing a definite assignment of the band system as $^2\Pi_{1/2}\leftarrow X\ ^2\Pi_{1/2}$.

Having determined the nature of the states involved in the transition, the observed rotational lines were then fit to the standard expression[7]

$$\nu=\nu_0+B'_v,J'(J'+1)\mp p'_v,(J'+1/2)/2 - B''_0J''(J''+1)\pm p''_0(J''+1/2)/2, \quad (3.1)$$

where the upper sign corresponds to e levels and the lower to f levels. In the case of AlZn it is impossible to establish the absolute parity of the observed levels with certainty, so the labels a and b are employed instead of e and f. The fit of the data to Eq. (3.1) confirmed that the transition is indeed $\Omega''=0.5\leftarrow\Omega''=0.5$ and that the bond does lengthen upon excitation ($r'_0>r''_0$).

The 2-0 band is very similar in appearance to the 0-0 band. In contrast, the data for the 3-0 band was collected under higher temperature source conditions. As a result of the greater population of the higher J levels, the R branch band head and Λ-doubling are more obvious. Rotational constants and band origins of all rotationally analyzed bands are given in Table II for all of the isotopic species resolved. The corresponding rotational line positions are available from the Physics Auxiliary Publication Service (PAPS) of the American Institute of Physics[8] or from the author (M.D.M.). From a linear fit of the B'_0, B'_2, and B'_3 constants (excluding the rotational constant of the perturbed 1-0 band), $B'_e(B\ ^2\Pi_{1/2}) = 0.116\,61 \pm 0.000\,15$ cm^{-1} and $\alpha'_e(B\ ^2\Pi_{1/2}) = 0.000\,32 \pm 0.000\,07$ cm^{-1} were determined for the $^{27}Al^{64}Zn$ species. Inverting the value of $B'_e(B\ ^2\Pi_{1/2})$, a value of $r'_e(B\ ^2\Pi_{1/2}) = 2.7603 \pm 0.0017$ Å is obtained. This is longer than the ground state bond length of $r''_0(X\ ^2\Pi) = 2.6957 \pm 0.0004$ Å, consistent with the development of a head in the R branch.

C. Rotationally resolved spectra of the $B\ ^2\Pi_{3/2}\leftarrow X\ ^2\Pi_{3/2}$ band system

The 0-0 band of the $B\ ^2\Pi_{3/2}\leftarrow X\ ^2\Pi_{3/2}$ band system was rotationally resolved under both hot and cold vaporization conditions. The colder of the two spectra had an intense Q branch, but the overall lack of intensity in the R and P branches prevented an accurate analysis. In contrast, the warmer spectrum displayed in Fig. 3 has sufficient assignable rotational lines for an excellent fit to be obtained. In addition, the Q branch is much weaker than in the cold spectrum, consistent with the rapid decline in intensity of Q lines with increasing J which is expected for an $\Omega'=3/2\leftarrow\Omega''=3/2$ transition. No Λ-doubling is evident in the spectrum, even in the highest J lines observed. This is consistent with the fact that in a $^2\Pi_{3/2}$ state the Λ-doubling is proportional to $(J-1/2)(J+1/2)(J+3/2)$ and is typically much smaller for low J than is found in the corresponding $^2\Pi_{1/2}$ state. (In Van Vleck's pure precession model,[7] for example, the Λ-doubling in a $^2\Pi_{3/2}$ state is smaller than that found in the $^2\Pi_{1/2}$ state by a factor proportional to B^2/A^2, which of the order of 10^{-6} in AlZn.) Accordingly, the spectrum was fitted to the formula

$$\nu=\nu_0+B'_v,J'(J'+1)-B''_0J''(J''+1). \quad (3.2)$$

Similar spectra were recorded for the 1-0 and 2-0 bands of the $B\ ^2\Pi_{3/2}\leftarrow X\ ^2\Pi_{3/2}$ system, leading to the rotational constants and band origins listed in Table II for the $^{27}Al^{64}Zn$ and $^{27}Al^{66}Zn$ isotopic modifications. From a linear fit of the B'_0, B'_1, and B'_2 constants $B'_e(B\ ^2\Pi_{3/2}) = 0.119\,28 \pm 0.000\,09$ cm^{-1} and $\alpha'_e(B\ ^2\Pi_{3/2}) = 0.001\,69 \pm 0.000\,06$ cm^{-1} were determined for the $^{27}Al^{64}Zn$ species. Inverting the value of $B'_e(B\ ^2\Pi_{3/2})$, a value of $r'_e(B\ ^2\Pi_{3/2}) = 2.7292 \pm 0.0010$ Å is obtained.

It is somewhat surprising that the B'_e values for the $B\ ^2\Pi_{1/2}$ and $B\ ^2\Pi_{3/2}$ states differ so significantly ($0.116\,61 \pm 0.000\,15$ vs $0.119\,28 \pm 0.000\,09$ cm^{-1}, respectively). This is unexpected because the spin–orbit splitting of the $B\ ^2\Pi$ state is about 101 cm^{-1} greater than that of the ground state (where the B''_0 values for the $X\ ^2\Pi_{1/2}$ and $X\ ^2\Pi_{3/2}$ components are more similar, at $0.122\,47 \pm 0.000\,06$ and $0.122\,06 \pm 0.000\,04$ cm^{-1}), making spin-uncoupling interactions between the $B\ ^2\Pi_{1/2}$ and $B\ ^2\Pi_{3/2}$ states too small to account for the differences in B'_e values. This suggests that one or both of the $B\ ^2\Pi$ components is perturbed by another state. Additional evidence for such an effect is the difference in vibrational constants found for the $B\ ^2\Pi_{1/2}$ and $B\ ^2\Pi_{3/2}$ substates, with $\omega'_e = 193.54$, $\omega'_ex'_e = 0.28$ cm^{-1} obtained for the former and $\omega'_e = 201.96$, $\omega'_ex'_e = 2.84$ cm^{-1} found for the latter. Likewise, the lifetime of the excited $B\ ^2\Pi_{3/2}$ $v'=0$ level has been measured as 247 ± 17 ns. Although this is not outrageously different from the lifetimes of the $B\ ^2\Pi_{1/2}$ $v'=0$ and $v'=2$ levels (197 ± 5 and 165 ± 44 ns, respectively), the difference appears to be real, again suggesting that one or both components of the $B\ ^2\Pi$ state are perturbed by another state.

D. Rotationally resolved spectrum of the $A\ \Omega=0.5\leftarrow X\ ^2\Pi_{1/2}$ band system

A weak blue-shaded band was found at 18 424 cm^{-1} and the lifetime of the upper state of this band was measured to be nearly a microsecond, much longer than that of the $B\ ^2\Pi_{1/2}$ state. This implies that the absorption oscillator

TABLE II. Fitted rotational constants for $^{27}Al^{64}Zn$ and $^{27}Al^{66}Zn$.[a]

Band system	Band	$^{27}Al^{64}Zn$	$^{27}Al^{66}Zn$
$B\ ^2\Pi_{1/2} \leftarrow X\ ^2\Pi_{1/2}$	0-0	$\nu_0 = 18\,506.035\,0(28)$	$\nu_0 = 18\,505.770\,0(29)$
		$B_0' = 0.116\,47(12)$	$B_0' = 0.116\,11(15)$
		$B_0'' = 0.122\,44(11)$	$B_0'' = 0.121\,65(14)$
		$p_0' = -0.007\,46(51)$	$p_0' = -0.014\,13(58)$
		$p_0'' = 0$ (fixed)	$p_0'' = 0$ (fixed)
	2-0	$\nu_0 = 18\,891.403\,9(32)$	$\nu_0 = 18\,889.600\,2(38)$
		$B_2' = 0.115\,72(16)$	$B_2' = 0.113\,95(22)$
		$B_0'' = 0.122\,57(17)$	$B_0'' = 0.121\,03(22)$
			$p_2' = -0.007\,83(119)$
			$p_0'' = 0$ (fixed)
	3-0	$\nu_0 = 19\,083.237\,1(27)$	$\nu_0 = 19\,080.533\,7(29)$
		$B_3' = 0.115\,62(23)$	$B_3' = 0.114\,36(18)$
		$B_0'' = 0.123\,06(20)$	$B_0'' = 0.121\,71(16)$
		$p_3' = -0.004\,33(34)$	$p_3' = -0.004\,37(41)$
		$p_0'' = 0$ (fixed)	$p_0'' = 0$ (fixed)
$B\ ^2\Pi_{3/2} \leftarrow X\ ^2\Pi_{3/2}$	0-0	$\nu_0 = 18\,605.892\,6(28)$	$\nu_0 = 18\,605.385\,8(37)$
		$B_0' = 0.118\,77(7)$	$B_0' = 0.118\,56(13)$
		$B_0'' = 0.121\,94(7)$	$B_0'' = 0.121\,15(12)$
	1-0	$\nu_0 = 18\,802.174\,1(15)$	$\nu_0 = 18\,801.176\,2(11)$
		$B_1' = 0.116\,40(5)$	$B_1' = 0.115\,22(4)$
		$B_0'' = 0.122\,10(5)$	$B_0'' = 0.120\,94(4)$
	2-0	$\nu_0 = 18\,992.773\,4(19)$	
		$B_2' = 0.115\,88(12)$	
		$B_0'' = 0.122\,18(13)$	
$A\ 0.5 \leftarrow X\ ^2\Pi_{1/2}$	2-0	$\nu_0 = 18\,424.294\,5(28)$	$\nu_0 = 18\,421.441\,0(26)$
		$B_2' = 0.141\,43(20)$	$B_2' = 0.140\,80(18)$
		$B_0'' = 0.121\,43(23)$	$B_0'' = 0.121\,06(21)$
		$p_2' = -0.041\,34(77)$	$p_2' = -0.039\,96(63)$
		$p_0'' = 0$ (fixed)	$p_0'' = 0$ (fixed)
Perturbed pair of bands	18 690 cm^{-1} band	$\nu_0 = 18\,690.271\,0(26)$	$\nu_0 = 18\,687.333\,1(27)$
		$B' = 0.129\,87(17)$	$B' = 0.131\,36(31)$
		$B_0'' = 0.122\,36(16)$	$B_0'' = 0.121\,77(41)$
		$p' = -0.028\,49(61)$	$p' = -0.029\,40(77)$
		$p_0'' = 0$ (fixed)	$p_0'' = 0$ (fixed)
	18 707 cm^{-1} band	$\nu_0 = 18\,706.533\,5(26)$	$\nu_0 = 18\,704.348\,1(31)$
		$B' = 0.127\,10(20)$	$B' = 0.123\,82(20)$
		$B_0'' = 0.122\,74(17)$	$B_0'' = 0.121\,16(25)$
		$p' = -0.022\,93(5)$	$p' = -0.018\,98(59)$
		$p_0'' = 0$ (fixed)	$p_0'' = 0$ (fixed)

[a]All constants reported in wave numbers (cm^{-1}) with 1σ error limits in parentheses.

strength of this transition is at least an order of magnitude reduced from that of the $B\ ^2\Pi_{1/2}$ state, indicating that the transition may be spin-forbidden. The blue-shaded nature of the band signifies that the bond shortens upon electronic excitation, a conclusion that is substantiated by the presence of a bandhead in the P branch in the rotationally resolved spectrum displayed in Fig. 4. In addition, Λ-doubling is immediately apparent in this band, where it is evident in the first R line and in the large separation between the heads of the two P branches. The presence of $R(0.5)$ and $P(1.5)$ again identifies the transition as an $\Omega' = 1/2 \leftarrow \Omega'' = 1/2$ band, and a least squares fit of the observed rotational lines to Eq. (3.1) provides the rotational constants listed in Table II for the $^{27}Al^{64}Zn$ and $^{27}Al^{66}Zn$ species. In addition, the upper state rotational constant, B_v', may be inverted to provide $r_v' = 2.5064 \pm 0.0018$ Å, which represents a considerable shortening of the bond relative to the ground state [$r_0''(X\ ^2\Pi = 2.6957 \pm 0.0004$ Å)]. Evidently this band represents excitation to a new $\Omega' = 0.5$ state, which we designate as the $A\ \Omega = 0.5$ state. Further, as will be proven in Sec. III G below, the measured isotope shift ($^{27}Al^{66}Zn - ^{27}Al^{64}Zn$) of

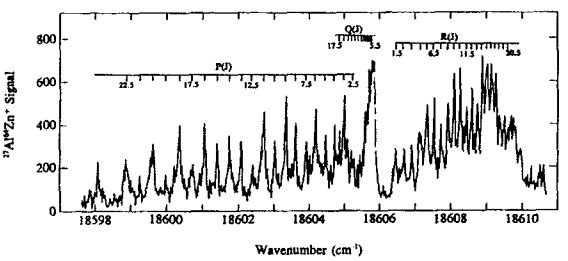

FIG. 3. Rotationally resolved spectrum of the 0-0 band of the $B\ ^2\Pi_{3/2} \leftarrow X\ ^2\Pi_{3/2}$ band system. This spectrum was collected under hotter source conditions than that of Fig. 2 and thus exhibits many more rotational lines.

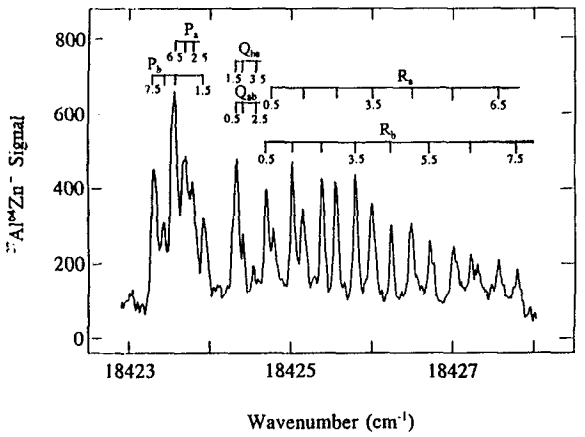

FIG. 4. Rotationally resolved spectrum of the 2-0 band of the $A\ \Omega=0.5\leftarrow X\ ^2\Pi_{1/2}$ band system. The sudden band head in the P-branch indicates that the bond shortens substantially upon electronic excitation, and a fit of the rotational lines provides $r_2' = 2.5064 \pm 0.0018$ Å. The Λ-doubling of the rotational lines is apparent at very low values of J.

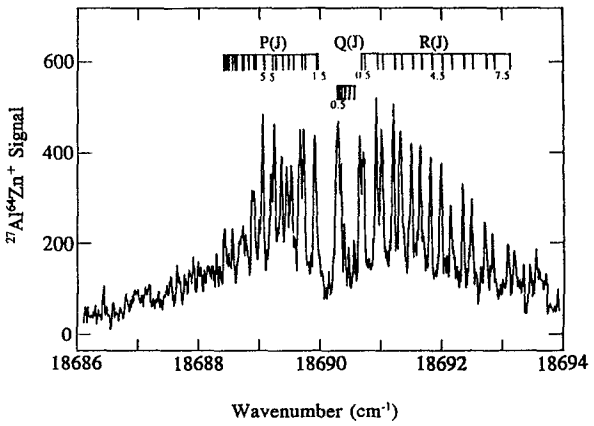

FIG. 5. Rotationally resolved scan over the 18 690 cm^{-1} band of $^{27}Al^{64}Zn$. As demonstrated in the text, the upper state of this transition is an approximately 54:46 mixture of the $A\ \Omega=0.5$, $v'=3$ and $B\ ^2\Pi_{1/2}$, $v'=1$ states. These states are mixed by a homogeneous spin–orbit perturbation with a perturbation matrix element of approximately 8 cm^{-1}.

-2.85 cm^{-1} suggests a tentative assignment of the 18 424 cm^{-1} feature as the 2-0 band of the $A\ \Omega=0.5\leftarrow X\ ^2\Pi_{1/2}$ system.

E. Rotationally resolved spectra of the perturbed 18 690 and 18 707 cm^{-1} bands

The measured lifetimes of the features at 18 690 and 18 707 cm^{-1} are found to be 301±32 and 259±23 ns, respectively. Given that the 1-0 band of the $B\ ^2\Pi_{1/2}\leftarrow X\ ^2\Pi_{1/2}$ system is expected in this region, and its lifetime would be expected to be approximately 200 ns, the appearance of two bands in this region with lengthened upper state lifetimes suggests that the $B\ ^2\Pi_{1/2}$, $v'=1$ level is perturbed strongly by another state which has a poorer radiative coupling to the ground state. In such a coupling mechanism the dark state gains oscillator strength, leading to a second vibronic feature in the spectrum. An obvious candidate for such a state is another vibronic level of the $A\ \Omega=0.5$ state. To investigate this possibility further, the two bands at 18 690 and 18 707 cm^{-1} were examined in high resolution.

A rotationally resolved scan over the 18 690 cm^{-1} band is displayed in Fig. 5, revealing a nearly symmetric rotational structure. Lambda doubling is also evident in both the P and R branches, even at low J-values. The obvious presence of $R(0.5)$ and $P(1.5)$ immediately identifies the band as an $\Omega'=1/2\leftarrow\Omega''=1/2$ band, as expected.

A similar rotationally resolved scan over the 18 707 cm^{-1} band is displayed in Fig. 6, again showing a nearly symmetric rotational structure without a strong tendency to form a head in either the P or the R branch. Lambda doubling is again evident in the P and R branches, even at low J-values. In its general appearance the 18 707 cm^{-1} band is quite similar to the 18 690 cm^{-1} band.

Both bands have been analyzed as $\Omega'=0.5\leftarrow\Omega''=0.5$ transitions, with the resulting rotational constants reported in Table II. The upper state rotational constants (B') and Λ-doubling parameters (p') for both bands are nearly identical and are almost precisely an average of the corresponding values of the $B\ ^2\Pi_{1/2}$ $v'=0$ and the $A\ \Omega=0.5$ $v'=2$ states. This strongly suggests that vibrational levels of these two states are nearly completely mixed by a homogeneous perturbation, which is probably due to the spin–orbit interaction. Furthermore, when one state perturbs another, the energy of one of the states is shifted by an amount that is equal and opposite in direction to the shift of the other state. Using this knowledge it is possible to predict the unperturbed frequency of the $A\ \Omega=0.5\leftarrow X\ ^2\Pi_{1/2}$ 3-0 band, from which a value of ω_e' of $\approx$279 cm^{-1} may be estimated for the $A\ \Omega=0.5$ state. This deperturbation analysis is discussed further in Sec. III G below.

F. Λ-doubling

A proper analysis of the Λ-doubling in the upper and lower states observed in AlZn requires careful thought because our experimental resolution (0.04 cm^{-1}) makes it difficult to determine the Λ-doubling parameters accurately. A

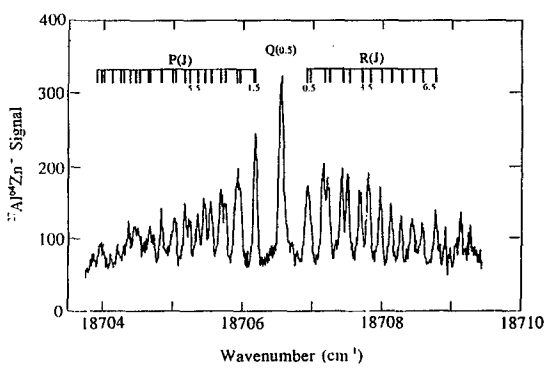

FIG. 6. Rotationally resolved scan of the 18 707 cm^{-1} band. This band also results from the perturbation between the $A\ \Omega=0.5$, $v'=3$ and $B\ ^2\Pi_{1/2}$, $v'=1$ states, which are almost completely mixed by a homogeneous spin–orbit perturbation.

major problem in this regard is the fact that the splittings in the individual lines were only measured reliably in the P branch for the $B\ ^2\Pi_{1/2} \leftarrow X\ ^2\Pi_{1/2}$ system (due to the band head in the R branch), and only in the R branch for the $A\ \Omega=0.5 \leftarrow X\ ^2\Pi_{1/2}$ system (due to the band head in the P branch). In such cases it is difficult if not impossible to independently determine p' and p'', because the splitting in the R or P branch grows linearly in J'', and is proportional to $(p'-p'')J''$. Thus, despite our observation of Λ-doubling in all of the observed bands involving $\Omega=1/2$ states, it is only in the perturbed 18 690 and 18 707 cm^{-1} bands, where Λ-doubling is cleanly observed in both the R and P branches, that reliable values of p' and p'' may be derived. Using Eq. (3.1) to analyze these perturbed bands demonstrated that the Λ-doubling parameter, p_0'', of the $X\ ^2\Pi_{1/2}$ ground state is small and poorly determined, with fitted values of $-0.000\,77(80)$ and $-0.002\,70(391)$ cm^{-1} for the 18 690 and 18 707 cm^{-1} bands of $^{27}Al^{64}Zn$, and $-0.002\,45(162)$ and $-0.005\,81(518)$ cm^{-1} for the corresponding bands of $^{27}Al^{66}Zn$ (Here the 1σ error limits are given in parentheses.) Given these small and indeterminate fitted values of p_0'', the choice was made to constrain p_0'' to zero in all of the band analyses reported here. It is perhaps not surprising that p'' is small; the only state close in energy to the $X\ ^2\Pi$ ground state (and therefore the major cause of Λ-doubling in the $X\ ^2\Pi$ ground state) is the $^2\Sigma^+$ state deriving from ground state atoms. The small value of p_0'' obtained here suggests a rather large splitting between the $X\ ^2\Pi$ state and the $^2\Sigma^+$ state, at least at the ground state internuclear separation of 2.6957 Å. Holding p_0'' equal to zero led to a negligible deterioration in the quality of the fit of the rotational lines, and reduced the uncertainties in the reported upper state Λ-doubling parameters significantly.

Another difficulty in this analysis is the determination of the absolute parity of the Λ-doublet levels. In the case of AlZn, the major contributor to the Λ-doubling of the ground $X\ ^2\Pi_r$ state is its interaction with the $^2\Sigma^+$ state arising from the same ground separated atom limit. Since this $^2\Sigma^+$ state lies above the $X\ ^2\Pi_r$ state, and we expect the matrix elements $a_+ \equiv \langle \pi|\hat{a}l^+|\sigma\rangle$ and $b \equiv \langle \pi|l^+|\sigma\rangle$ to have the same sign, one would expect the Λ-doubling parameter p_0'' to be negative, with f levels lying below e levels.[7] If the magnitude of this parameter had been well-determined in the fits of the rotational bands, this would have allowed a determination of the proper e,f labeling scheme. Unfortunately this is impossible at the present level of resolution, so the more conservative a,b labeling scheme is used instead.

With the value of p_0'' constrained to be zero, fits of the observed bands yield fairly small Λ-doubling parameters for the vibronic levels of the $B\ ^2\Pi_{1/2}$ state of $p_0' = -0.007\,46(51)$ and $p_3' = -0.004\,33(34)$ cm^{-1} for $^{27}Al^{64}Zn$ and $p_0' = -0.014\,13(58)$, $p_2' = -0.007\,83(119)$, and $p_3' = -0.004\,37(41)$ cm^{-1} for $^{27}Al^{66}Zn$. The fitted values of p_v' (obtained holding $p_0'' = 0$) for the perturbed 18 690 and 18 707 cm^{-1} bands are much larger in absolute magnitude, giving $-0.028\,49(61)$ and $-0.022\,93(55)$ cm^{-1} for $^{27}Al^{64}Zn$, and $-0.029\,40(77)$ and $-0.018\,98(59)$ cm^{-1} for $^{27}Al^{66}Zn$, respectively. Finally, the fitted value of p_2' obtained from the rotationally resolved scan over the 2-0 band of the $A\ \Omega=0.5 \leftarrow X\ ^2\Pi_{1/2}$ system at 18 634 cm^{-1} is even larger in magnitude, with $p_2' = -0.041\,34(77)$ for $^{27}Al^{64}Zn$ and $p_2' = -0.039\,96(63)$ cm^{-1} for $^{27}Al^{66}Zn$. Again, 1σ error limits are provided in parentheses.

Although these values are undoubtedly not accurate because of experimental difficulties in resolving all of the lines and our constraint of p_0'' to zero, we feel confident in the trend that is established. The $A\ \Omega=0.5$ state of AlZn displays a larger Λ-doubling than does the $B\ ^2\Pi_{1/2}$ state, which in turn displays a larger Λ-doubling than does the ground state. Moreover, the Λ-doubling of the perturbed pair of levels at 18 690 and 18 707 cm^{-1} is intermediate in magnitude to that found for the $A\ \Omega=0.5$, $v=2$ level and the various levels of the $B\ ^2\Pi_{1/2}$ state. This supports our interpretation of these levels as arising from a perturbation between the $v'=1$ level of the $B\ ^2\Pi_{1/2}$ state and the $v'=3$ level of the $A\ \Omega=0.5$ state. Furthermore, if we estimate the unperturbed value of $p_1'(B\ ^2\Pi_{1/2})$ by interpolating between the values given above, values of $-0.006\,42$ and $-0.010\,98$ cm^{-1} are obtained for $^{27}Al^{64}Zn$ and $^{27}Al^{66}Zn$, respectively. If these are averaged with the corresponding value for the $v'=3$ level of the $A\ \Omega=0.5$ state (estimated as equal to that of the $A\ \Omega=0.5$, $v'=2$ level) we can obtain estimates of the average of p' values for the perturbed pair of states. The fact that these averaged values ($-0.023\,88$ and $-0.025\,47$ cm^{-1} for $^{27}Al^{64}Zn$ and $^{27}Al^{66}Zn$, respectively) are in close agreement with the average of the p' values actually found for the two perturbed bands ($-0.025\,71$ and $-0.024\,19$ cm^{-1} for $^{27}Al^{64}Zn$ and $^{27}Al^{66}Zn$, respectively) substantiates the assignment of the perturbation as $A\ \Omega=0.5$, $v'=3 \sim B\ ^2\Pi_{1/2}$, $v'=1$. Furthermore, it also establishes that the sign of p' (which is undetermined in our present study because of the difficulty in establishing the absolute parity of the levels) is the same in both the $A\ \Omega=0.5$ and $B\ ^2\Pi_{1/2}$ states. Thus in both states either the f levels lie below the e levels or vice versa, but in any event the ordering of the e/f levels is the same in both states.

G. Deperturbation analysis of the 18 690 and 18 707 cm^{-1} bands

The deperturbation of the 18 690 and 18 707 cm^{-1} bands is greatly facilitated by the high resolution analyses of the $B\ ^2\Pi_{1/2} \leftarrow X\ ^2\Pi_{1/2}$ 0-0, 2-0, and 3-0 bands for both the $^{27}Al^{64}Zn$ and the $^{27}Al^{66}Zn$ isotopic modifications. By fitting the band origins of these bands to the formula

$$\nu_{v'-0} = \nu_{00} + \omega_e' v' - \omega_e' x_e' (v'^2 + v') \tag{3.3}$$

one may obtain accurate values of ν_{00}, ω_e', and $\omega_e' x_e'$, which in turn may be used to predict the frequency at which the 1-0 band of the $B\ ^2\Pi_{1/2} \leftarrow X\ ^2\Pi_{1/2}$ transition would lie if the perturbation were absent. Through this procedure the 18 706.534 (18 704.348) cm^{-1} band for $^{27}Al^{64}Zn$ ($^{27}Al^{66}Zn$) is found to lie 7.531 cm^{-1} (6.335 cm^{-1}) above the predicted frequency of the $B\ ^2\Pi_{1/2} \leftarrow X\ ^2\Pi_{1/2}$ 1-0 band. This further implies that the 18 690.271 (18 687.333) cm^{-1} band has been shifted lower in frequency as a result of the perturbation, assuming that only two states are involved. This finally allows the energies of the deperturbed levels to be fixed as

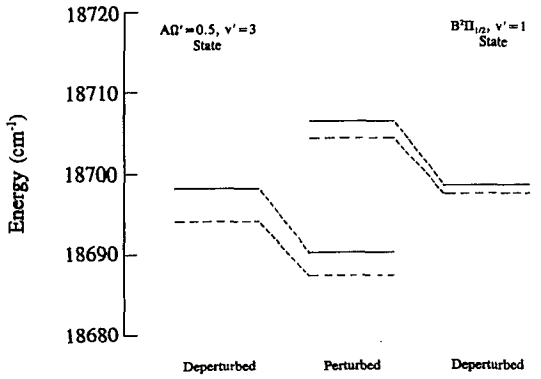

FIG. 7. Plot of the effect of the homogeneous spin–orbit perturbation between the $A\ \Omega=0.5$, $v'=3$ and the $B\ ^2\Pi_{1/2}$, $v'=1$ states illustrating the effect on the measured isotope shifts. The $^{27}Al^{64}Zn$ energy levels are drawn as solid lines while the $^{27}Al^{66}Zn$ energy levels are depicted with dashed lines. Both are measured relative to the $X\ ^2\Pi_{1/2}$, $v''=0$ level of the corresponding species. The measured energy levels are in the central column and the deperturbed levels are displayed in the left and right columns. The perturbation causes the measured isotope shift for the 18 690 cm^{-1} band to be reduced and that of the 18 707 cm^{-1} band to be increased as compared to their unperturbed values.

18 697.802 (for the $A\ \Omega=0.5$, v' state) and 18 699.003 cm^{-1} (for the $B\ ^2\Pi_{1/2}$, $v'=1$ state) above the $v''=0$ level of the $X\ ^2\Pi_{1/2}$ state for $^{27}Al^{64}Zn$ (and 18 693.668 and 18 698.013 cm^{-1}, respectively, above the $v''=0$ level of the $X\ ^2\Pi_{1/2}$ state for $^{27}Al^{66}Zn$). A pictorial representation of both the actual and deperturbed levels is displayed in Fig. 7.

These deperturbed energies are satisfying because the resulting isotope shifts $[\nu(^{27}Al^{64}Zn)-\nu(^{27}Al^{66}Zn)]$ for the v'-0 bands of the $B\ ^2\Pi_{1/2}\leftarrow X\ ^2\Pi_{1/2}$ system now fall in line as 0-0, 0.265 cm^{-1}; 1-0, 0.990 cm^{-1} (deperturbed); 2-0, 1.804 cm^{-1}; 3-0, 2.703 cm^{-1}. Assuming that the perturber is a vibrational level of the $A\ \Omega=0.5$ state, it is also satisfying that the isotope shifts of the band at 18 424.294 cm^{-1} and the second deperturbed band now correspond to 2.854 and 4.134 cm^{-1}, respectively. Assuming that these two bands correspond to sequential vibrational levels of the $A\ \Omega=0.5$ state, the isotope shift equation relating isotopic species i and j,

$$\nu^i_{v'-0}-\nu^j_{v'-0}=[(v'+1/2)\omega'_{ei}-\omega''_{ei}/2][1-(\mu_i/\mu_j)^{1/2}] -[(v'+1/2)^2\omega'_{ei}x'_{ei}-\omega''_{ei}x''_{ei}/4] \times[1-(\mu_i/\mu_j)] \quad (3.4)$$

may be used to establish the vibrational numbering of the $A\ \Omega=0.5$ state unambiguously. Using estimated values of ω'_e = 279 cm^{-1} (based on the difference in frequency between the $A\ \Omega=0.5$, $v'=2$ and the deperturbed $A\ \Omega=0.5$, $v'=3$ levels), an estimated value of $\omega'_e x'_e$ = 0.8 cm^{-1}, ω''_e = 155 cm^{-1} (as determined from a vibrational hot band analysis of the $B\ ^2\Pi_{1/2}\leftarrow X\ ^2\Pi_{1/2}$ band system), and $\omega''_e x'_e$ = 1 cm^{-1} (as a reasonable guess), we find expected isotope shifts $[\nu(^{27}Al^{66}Zn)-\nu(^{27}Al^{64}Zn)]$ for bands of the $A\ \Omega=0.5\leftarrow X\ ^2\Pi_{1/2}$ band system of −0.280 cm^{-1} (0-0 band), −1.522 cm^{-1} (1-0 band), −2.750 cm^{-1} (2-0 band), −3.964 cm^{-1} (3-0 band), and −5.164 cm^{-1} (4-0 band). Clearly, the observed bands, with isotope shifts of −2.854 and −4.134 cm^{-1} (deperturbed) correspond to the 2-0 and 3-0 bands of the $A\ \Omega=0.5\leftarrow X\ ^2\Pi_{1/2}$ system, respectively, and the perturbation is between the $A\ \Omega=0.5$, $v'=3$ and the $B\ ^2\Pi_{1/2}$, $v'=1$ levels.

Knowing the deperturbed energy levels as well as the final observed levels, one may calculate the magnitude of the perturbation matrix element which is responsible for their mixing. This may be done independently for $^{27}Al^{64}Zn$ and $^{27}Al^{66}Zn$, yielding values of 8.109 and 8.226 cm^{-1} for H_{12}, respectively. The close agreement between these two values provides validation for the deperturbation method, particularly in the use of the two-state model. This perturbation matrix element, in turn, has two components, a vibrational factor (approximated by the Franck–Condon overlap of the $A\ \Omega=0.5$ $v'=3$ and $B\ ^2\Pi_{1/2}$, $v'=1$ vibrational wave functions) and an electronic matrix element. An approximate Franck–Condon calculation provides a value of the vibrational factor $\langle B\ ^2\Pi_{1/2},v'=1|A\ \Omega=0.5,v'=3\rangle$ of 0.25, implying that the electronic matrix element coupling the $B\ ^2\Pi_{1/2}$ and $A\ \Omega=0.5$ states is roughly 33 cm^{-1}. Combined with the long lifetime of the $A\ \Omega=0.5$, $v'=2$ level (which may be limited by predissociation rather than fluorescence), our inability to observe other vibrational levels of the $A\ \Omega=0.5$ state strongly suggests that the $A\ \Omega=0.5$ state is primarily quartet ($S=3/2$) in character. Spin–orbit selection rules governing the coupling of a $^2\Pi$ state to a quartet state then require that the $A\ \Omega=0.5$ state must be a $^4\Sigma_{1/2}$, $^4\Pi_{1/2}$, or $^4\Delta_{1/2}$ state.[7]

Having deduced the energies of the deperturbed energy levels and the magnitude of the perturbation matrix element, it now becomes possible to determine the degree to which the $A\ \Omega=0.5$, $v'=3$ and $B\ ^2\Pi_{1/2}$, $v'=1$ states are mixed in the upper levels of the perturbed bands. For the $^{27}Al^{64}Zn$ isotopic species the upper state of the 18 690 cm^{-1} band is found to have 54% $A\ \Omega=0.5$ character and 46% $B\ ^2\Pi_{1/2}$ character while for the $^{27}Al^{66}Zn$ isotopic modification the upper state of the 18 687 cm^{-1} band has 63% $A\ \Omega=0.5$ character and 37% $B\ ^2\Pi_{1/2}$ character. These percentages are exactly reversed when one considers the higher frequency, 18 707 cm^{-1} band, as is required for the two state perturbation problem. The fact that the A and B states are less thoroughly mixed in the $^{27}Al^{66}Zn$ species is a simple result of the fact that the deperturbed levels are further apart in energy in this species, as is shown in Fig. 7.

The nearly 50–50 mix of A and B state character nicely explains why the fitted rotational constants (both B' and p') of the perturbed excited states lie so close to the average of the $A\ \Omega=0.5$, $v'=2$ and $B\ ^2\Pi_{1/2}$, $v'=0$ values. In fact, using the percent A and B character listed above and the estimated B values of the deperturbed $A\ \Omega=0.5$, $v'=3$ and $B\ ^2\Pi_{1/2}$, $v'=1$ levels [taken as equal to the measured value of $B'_2(A\ \Omega=0.5)$ and the average of the $B'_0(B\ ^2\Pi_{1/2})$ and $B'_2(B\ ^2\Pi_{1/2})$ values, respectively], it is possible to predict the B values expected for the upper states of the 18 690 and 18 707 cm^{-1} bands. This procedure gives predictions of 0.129 72 and 0.127 85 cm^{-1} for the upper state of the 18 690 and 18 707 cm^{-1} bands in $^{27}Al^{64}Zn$ (compared to measured values of 0.129 87 and 0.127 10 cm^{-1}, respectively) and 0.131 33 and 0.124 81 cm^{-1} in $^{27}Al^{66}Zn$ (compared to mea-

TABLE III. Electronic states of $^{27}Al^{64}Zn$.[a]

State	T_0 (cm^{-1})	ω_e (cm^{-1})	$\omega_e x_e$ (cm^{-1})	B_e (cm^{-1})	α_e (cm^{-1})	r_e (Å)	τ (ns)
$B\ ^2\Pi_{3/2}$	18 605.892 6(28)+x	201.96	2.84	0.119 28 (9)	0.001 69(6)	2.729(1)	247 (17)
$B\ ^2\Pi_{1/2}$	18 506.035 0(28)	193.54	0.28	0.116 61(15)	0.000 32(7)	2.760(2)	197 (5)
$A\ \Omega=0.5$	~17 870[b]	$\Delta G_{5/2}$=273.5		B_2=0.141 43 (20)		2.506 (2)[c]	977 (244)
$X\ ^2\Pi_{3/2}$	x	$\Delta G_{1/2}$=154.5 (2.3)		B_0=0.122 06 (4)		2.6957 (4)[d]	
$X\ ^2\Pi_{1/2}$	0.000	$\Delta G_{1/2}$=153.4 (0.7)		B_0=0.122 47 (6)			

[a]1σ error limits are provided in parentheses and correspond to the last digit(s) in the corresponding values.
[b]Calculated assuming ω_e=279 cm^{-1} and $\omega_e x_e$=0.8 cm^{-1}.
[c]This value is r_2, not r_e.
[d]This value is an average of the r_0 values obtained for the $X\ ^2\Pi_{1/2}$ and $X\ ^2\Pi_{3/2}$ states.

sured values of 0.131 36 and 0.123 82 cm^{-1}, respectively). The close agreement of these results substantiates the validity of the deperturbation analysis. With the completion of this analysis, the known electronic states of $^{27}Al^{64}Zn$ are summarized in Table III.

H. Ionization energy of AlZn

In using resonant two-photon ionization to probe the spectroscopy of AlZn the $A\ \Omega=0.5 \leftarrow X\ ^2\Pi_{1/2}$ 2-0 transition at 18 424 cm^{-1} (2.284 eV) was observed using KrF excimer radiation (4.997 eV) for photoionization. This places the ionization energy of AlZn below 7.281 eV. In turn, the fact that KrF radiation is suitable for the second, ionizing photon sets the lower limit on the ionization energy of AlZn as 4.997<IE(AlZn). Studies with ArF excimer radiation have further indicated that AlZn is one photon ionized at this wavelength, thereby loosely bracketing the ionization energy of AlZn as 4.997<IE(AlZn)<6.42 eV.

IV. DISCUSSION

The present gas phase analysis has unambiguously determined the ground state of AlZn as $X\ ^2\Pi_{1/2}$, with a ground state electronic configuration of $3s^2_{Al}4s^2_{Zn}\pi^1$, $^2\Pi_{1/2}$, where the π orbital is primarily $3p\pi_{Al}$ in character, although some $4p\pi_{Zn}$ character is undoubtedly present as well. As was found from the theoretical studies reported for AlCa in the preceding paper,[3] it is likely that there is some partial transfer of $4s_{Zn}$ electron density into the empty $3p\sigma_{Al}$ orbital, although electronegativity differences make this dative bonding interaction much less favorable in AlZn than in AlCa. For this reason we believe AlZn is probably less strongly bound than is AlCa. This is consistent with the greater difficulty in preparing a molecular beam of AlZn as compared to AlCa.

In comparing AlZn to AlCa one is struck by the substantial difference in bond lengths of these isovalent molecules. The bond length of ground state AlZn (2.6957±0.0004 Å) is 0.452 Å shorter than that of AlCa (3.1479±0.0010 Å),[3] a result that is directly related to the decrease in atomic radius in going from calcium (r_{Ca}=1.97 Å) to zinc (r_{Zn}=1.33 Å).[9] This decrease in atomic radius results from the substantial contraction of the $4s$ orbital as one moves across the $3d$ series, which may be quantified by the radial expectation values $\langle r_{4s}\rangle$ calculated in a numerical Dirac–Fock method by Desclaux to be $\langle r_{4s}\rangle_{Ca}$=2.22 Å and $\langle r_{4s}\rangle_{Zn}$=1.51 Å.[10]

Like the closed subshell Zn and Ca atoms, the rare gases Ar and Kr also combine with Al to form complexes with $^2\Pi_{1/2}$ ground states.[11–13] The rare gas species, however, have considerably longer ground state bond lengths because the bonding in these species is dominated by dispersion forces. As a result the AlAr and AlKr molecules may be classified as van der Waals complexes. The equilibrium internuclear separation of AlAr,[12] for example, has been experimentally determined as r''_e = 3.79 ± 0.01 Å while that of AlKr (Ref. 13) is r''_e = 3.84 ± 0.01 Å. We may use these values to test for the existence of chemical bonding in AlZn.

Assuming additivity of bond lengths in van der Waals complexes, the bond lengths of Ar_2 (r''_e = 3.80 Å),[14] AlAr (r''_e = 3.79 Å),[12] and ZnAr (r''_e = 4.18 Å),[15] may be used to establish van der Waals radii of 1.90, 1.89, and 2.28 Å for Ar, Al, and Zn, respectively. If the AlZn molecule were bonded primarily by van der Waals forces one would then expect a bond length of roughly 4.17 Å. The large discrepancy between this value and the measured bond length of 2.69 Å demonstrates convincingly that there is indeed some type of chemical bonding occurring in diatomic AlZn. This probably results from a weak σ donation from the filled $4s$ orbital of zinc into the empty $3p\sigma$ orbital of aluminum, with concomitant weak back-donation of $3p\pi$ electrons from aluminum into the $4p\pi$ orbital of zinc.

The nature of the chemical bonding in the excited $B\ ^2\Pi$ state may be considered by first establishing the excited separated atom limits that can generate $^2\Pi$ states. The lowest limits capable of generating such states are the Al $3s^23d^1$, ^2D+Zn $4s^2$, ^1S limit at 32 436 cm^{-1}, the Al $3s^23p^1$, $^2P^0$+Zn $4s^14p^1$, $^3P^0$ limit at ≈32 500 cm^{-1}, and the Al $3s^24p^1$, $^2P^0$+Zn $4s^2$, ^1S limit at ≈32 950 cm^{-1}. Given that the $B\ ^2\Pi$ state of AlZn correlates to one of these separated atom limits, the observation of the B–X 0-0 band at 18 506 cm^{-1} implies that the bond strength of the excited $B\ ^2\Pi$ state exceeds that of the $X\ ^2\Pi$ ground state by at least 13 930 cm^{-1} (32 436–18 506 cm^{-1}). Given this fact, it seems most likely that the B state correlates to the Al $3s^23p^1$, $^2P^0$+Zn $4s^14p^1$, $^3P^0$ limit, which opens the $4s$ subshell of zinc permitting strong σ-bonding to occur. The Al $3s^24p^1$, $^2P^0$+Zn $4s^2$, ^1S limit may certainly be excluded from consideration, because the $^2\Pi$ state resulting from this limit corresponds simply to promotion of the weakly bonding π electron to a Rydberg π orbital which is certainly nonbonding in character. Likewise it is difficult to imagine how at least 13 930 cm^{-1} (1.73 eV) of additional bonding could be obtained from an Al $3s^23d^1$, ^2D+Zn $4s^2$, ^1S interaction, since the $3d\pi_{Al}$ orbital would be at best only slightly

more capable of a bonding interaction with the empty $4p\pi$ orbital of zinc than the $3p\pi_{Al}$ orbital. On this basis we correlate the $B\ ^2\Pi$ state with the Al $3s^2 3p^1$, $^2P^0$+Zn $4s^1 4p^1$, $^3P^0$ separated atom limit.

Low-lying quartet states that are candidates for the $A\ \Omega=0.5$ state of AlZn must derive from either the Al $3s^1 3p^2$, ^4P+Zn $4s^2$, ^1S limit at $\approx$29 070 cm^{-1} or from the Al $3s^2 3p^1$, $^2P^0$+Zn $4s^1 4p^1$, $^3P^0$ limit at $\approx$32 500 cm^{-1}. The former limit leads to $^4\Pi$ and $^4\Sigma^-$ states while the latter gives $^4\Sigma^+(2)$, $^4\Sigma^-$, $^4\Pi(2)$, and $^4\Delta$ states, all of which have the requisite symmetry to undergo spin–orbit perturbation with the $B\ ^2\Pi$ state. Again, the A state must be strongly bound, with a bond strength at least 11 000 cm^{-1} (29 070–18 000) (1.36 eV) greater than the ground state. As in the $B\ ^2\Pi$ state, this greatly enhanced bond strength arises because a hole has been opened in a filled s orbital. In this case it could be either the $3s_{Al}$ or the $4s_{Zn}$ orbital that has been opened, in either case resulting in greatly improved σ-bonding.

V. CONCLUSION

The present spectroscopic investigation of AlZn provides the first study, spectroscopic or otherwise, to be performed on this diatomic species. High resolution resonant two-photon ionization spectroscopy has allowed the ground state of the molecule to be unambiguously determined as $X\ ^2\Pi_{1/2}$, similar to the ground states of the diatomic aluminide species, AlCa,[3] AlAr,[11,12] and AlKr.[12,13] These studies have confirmed the preferential orientation of the Al $3p$ electron to be $3p\pi$ in the presence of another filled subshell atom. In the present study of AlZn two electronic states, labeled the $A\ \Omega=0.5$ and $B\ ^2\Pi$ states, have been characterized and a homogeneous spin–orbit perturbation between two vibrational levels of these states has been analyzed. A weighted least squares value for the ground state bond length of AlZn has been determined as $r_0''(X\ ^2\Pi) = 2.6957 \pm 0.0004$ Å.

The bonding in AlZn appears to be substantially different than that proposed for AlCu (Ref. 1) and AlNi,[2] where covalent interaction between the $3p\sigma$ electron of aluminum and a lone $4s$ electron of the transition metal leads to a strong two-electron σ^2 bond. In contrast, it is rather similar to the bonding in AlCa.[3] It is hoped that knowledge gained through the study of AlZn and AlCa (Ref. 3) will allow us to rationalize the bonding interactions which occur in other transition metal aluminides, particularly species such as AlSc and AlMn. The scandium and manganese transition metal partners in these diatomic transition metal aluminides possess large $3d \leftarrow 4s$ promotion energies which may obstruct the formation of a two electron $3p\sigma_{Al}$–$4s\sigma_M$ σ^2 bond, leading to a preferential $p\pi$ orientation as the aluminum atom approaches the scandium or manganese atom. Further studies are currently underway to test this hypothesis.

ACKNOWLEDGMENTS

We thank Professor William H. Breckenridge for the use of the intracavity étalon employed in the high resolution studies and for a number of stimulating conversations regarding AlZn and its comparison to AlAr and AlKr. We also thank Caleb A. Arrington for his expert preparation of the AlZn alloy required for these studies and John G. Kaup for his help in the evaluation of Franck–Condon factors in the $B\ ^2\Pi$, $v'=1 \sim A\ \Omega=0.5$, $v'=3$ perturbation matrix element. Research support from the National Science Foundation under Grant No. CHE-9215193 is gratefully acknowledged. Acknowledgement is also made to the Eastman Kodak Company for a fellowship, and to the donors of the Petroleum Research Fund, administered by the American Chemical Society, for partial support of this research.

[1] J. M. Behm, C. A. Arrington, J. D. Langenberg, and M. D. Morse, J. Chem. Phys. **99**, 6394 (1993).
[2] J. M. Behm, C. A. Arrington, and M. D. Morse, J. Chem. Phys. **99**, 6409 (1993).
[3] J. M. Behm, M. D. Morse, A. I. Boldyrev, and J. Simons, J. Chem. Phys. **101**, 5441 (1994).
[4] C. E. Moore, Natl. Bur. Stand. Circ. 467 (1971).
[5] S. Gerstenkorn and P. Luc, *Atlas du Spectre d'Absorption de la Molécule d'Iode* (CNRS, Paris, 1978); S. Gerstenkorn and P. Luc, Rev. Phys. Appl. **14**, 791 (1979).
[6] E. U. Condon and G. H. Shortley, *The Theory of Atomic Spectra* (Cambridge University, Cambridge, 1970).
[7] H. Lefebvre-Brion and R. W. Field, *Perturbations in the Spectra of Diatomic Molecules* (Academic, Orlando, 1986).
[8] See AIP document No. PAPS JCPSA-101-5454-3 for 3 pages of absolute line positions. Order by PAPS number and journal reference from American Institute of Physics, Physics Auxiliary Publication Service, Carolyn Gehlbach, 500 Sunnyside Boulevard, Woodbury, New York 11797-2999. The price is $1.50 for each microfiche (98 pages) or $5.00 for photocopies of up to 30 pages, and $0.15 for each additional page over 30 pages. Airmail additional. Make checks payable to the American Institute of Physics.
[9] R. W. G. Wyckoff, *Crystal Structures*, 2nd ed. (Interscience, New York, 1963).
[10] J. P. Desclaux, At. Data Nucl. Data **12**, 311 (1973).
[11] C. L. Callender, S. A. Mitchell, and P. A. Hackett, J. Chem. Phys. **90**, 5252 (1989).
[12] M. J. McQuaid, J. L. Gole, and M. C. Heaven, J. Chem. Phys. **92**, 2733 (1990).
[13] Z.-W. Fu, S. Massick, J. G. Kaup, O. B. d'Azy, and W. H. Breckenridge, J. Chem. Phys. **97**, 1683 (1992).
[14] D. E. Woon, J. Chem. Phys. **100**, 2838 (1994).
[15] I. A. Wallace, R. R. Bennett, and W. H. Breckenridge, Chem. Phys. Lett. **153**, 127 (1988).